Endocrine, Metabolic & Immune Disorders - Drug Targets, 2020, *20*, 771-780

RESEARCH ARTICLE

Insulin Resistance in Apolipoprotein M Knockout Mice is Mediated by the Protein Kinase Akt Signaling Pathway

Shuang Yao[1], Jun Zhang[1], Yuxia Zhan[1], Yuanping Shi[1], Yang Yu[1], Lu Zheng[1], Ning Xu[2,*] and Guanghua Luo[1,*]

[1]*Comprehensive Laboratory, The Third Affiliated Hospital of Soochow University, Changzhou, China;* [2]*Section of Clinical Chemistry and Pharmacology, Institute of Laboratory Medicine, Lunds University, Lund, Sweden*

Abstract: ***Background:*** Previous clinical studies have suggested that apolipoprotein M (apoM) is involved in glucose metabolism and plays a causative role in insulin sensitivity.

Objective: The potential mechanism of apoM on modulating glucose homeostasis is explored and differentially expressed genes are analyzed by employing *ApoM* deficient (*ApoM*$^{-/-}$) and wild type (WT) mice.

Methods: The metabolism of glucose in the hepatic tissues of high-fat diet *ApoM*$^{-/-}$ and WT mice was measured by a glycomics approach. Bioinformatic analysis was applied for analyzing the levels of differentially expressed mRNAs in the liver tissues of these mice. The insulin sensitivity of *ApoM*$^{-/-}$ and WT mice was compared using the insulin tolerance test and the phosphorylation levels of protein kinase Akt (AKT) and insulin stimulation in different tissues were examined by Western blot.

Results: The majority of the hepatic glucose metabolites exhibited lower concentration levels in the *ApoM*$^{-/-}$ mice compared with those of the WT mice. Gene Ontology (GO) classification and Kyoto Encyclopedia of Genes and Genomes (KEGG) enrichment analysis indicated that *ApoM* deficiency affected the genes associated with the metabolism of glucose. The insulin tolerance test suggested that insulin sensitivity was impaired in *ApoM*$^{-/-}$ mice. The phosphorylation levels of AKT in muscle and adipose tissues of *ApoM*$^{-/-}$ mice were significantly diminished in response to insulin stimulation compared with those noted in WT mice.

Conclusion: *ApoM* deficiency led to the disorders of glucose metabolism and altered genes related to glucose metabolism in mice liver. *In vivo* data indicated that apoM might augment insulin sensitivity by AKT-dependent mechanism.

ARTICLE HISTORY

Received: July 24, 2019
Revised: September 12, 2019
Accepted: September 13, 2019

DOI:
10.2174/1871530319666191023125820

Keywords: Apolipoprotein M, glucose metabolism, microarray, insulin resistance, protein kinase akt phosphorylation, type 2 diabetes.

1. INTRODUCTION

Type 2 diabetes (T2D) is an epidemic disease, affecting the health of millions of subjects worldwide [1]. Accordingly, glucose metabolism disorders facilitate profound disturbances in the metabolism of lipids and amino acids and inflict long-lasting injury effects on different tissues and organs [2]. The regulation of insulin sensitivity is a critical issue in maintaining glucose homeostasis and alleviating both T2D and obesity [3]. High-density lipoprotein (HDL) can regulate glucose homeostasis by enhancing insulin sensitivity and increasing insulin synthesis and secretion [4-8]. Apolipoprotein M (ApoM) is a member of lipocalin superfamily that is associated with the formation of pre-β HDL [9, 10]. This lipoprotein was discovered approximately 20 years ago [11]. However, the function and regulating mechanism of apoM in glucose homeostasis have not been fully understood . The association between apoM and glucose metabolism has been previously investigated in several research studies [12-14]. Certain SNPs of the *APOM* gene, such as the T-778C have been shown to be associated with type 1 and 2 Mellitus [15]. ApoM serum levels have also been shown to function as a marker for maturity-onset diabetes of the young 3 (MODY3) [16], which is characterized by mutations in the *hepatocyte nuclear factor-1 α (HNF-1α)* gene. In addition, it has been shown that *Hnf-1α*$^{-/-}$ mice exhibit undetectable plasma apoM levels [17]. However, the precise underlying mechanisms for these epidemiological associations have not been elucidated yet.

* Address correspondence to these two authors at the Comprehensive Laboratory, the Third Affiliated Hospital of Soochow University, 213003, Changzhou, China; Tel: +86-0519-68870619; E-mail: shineroar@163.com, and the Section of Clinical Chemistry & Pharmacology, Institute of Laboratory Medicine, Lunds University, S-22185 Lund, Sweden;
E-mail: ning.xu@med.lu.se

2212-3873/20 $65.00+.00

A previous study has suggested that higher plasma apoM concentration is consistent with higher insulin sensitivity [18]. *ApoM* gene expression in obese mice is markedly decreased [19], and weight-reducing diets can increase *ApoM* gene expression and secretion in adipose tissues [18]. Notably, apoM has been deemed an important component of rare adipokines associated with healthy metabolic status [18]. *APOM* gene polymorphism is also related to the metabolism of HDL in obese Korean male adults [20]. The aforementioned studies have shown that apoM may play a causative role in insulin sensitivity. To comprehensively understand the role of insulin and examine the potential mechanism of action in lipid disorders, a thorough investigation of the signaling cascades of insulin is required. AKT is the main pathway involved in insulin-associated lipid and glucose metabolism [21, 22]. Under normal conditions, insulin activates the AKT signaling pathway, which finally leads to an increase in glucose utilization and a decrease in gluconeogenesis in muscle or adipose tissues [23, 24]. Impaired AKT signaling is one of the main causes of insulin resistance, which in turn exacerbates AKT signaling [25]. It is reported that apoM together with sphingosine-1-phosphate inhibits oxidatively modified low-density lipoprotein induced inflammation by activating the AKT pathway [26, 27]. A previous study also demonstrated that overexpressing apoM might promote activation of AKT signaling pathways in lung cancer cells [28]. Therefore, it was supposed that apoM might improve insulin sensitivity by enhancing AKT activation.

Briefly, glucose metabolism and the differential genes were measured in the liver tissues of *ApoM*$^{-/-}$ mice who were fed a high-fat diet by means of metabonomic approach, microarray and bioinformatic analysis. Furthermore, the insulin sensitivity of *ApoM*$^{-/-}$ and WT mice was compared with the phosphorylation levels of AKT following insulin stimulation in different tissues.

2. MATERIALS AND METHODS

2.1. Animals

ApoM$^{-/-}$ mice (C57BL/6J) were employed at the animal research institute of the Nanjing University (Jiangsu) [29]. The genotypes of parental mice and their offsprings were analyzed by polymerase chain reaction as described previously [30]. The conditions for a regular and stress-free life period were provided, including a moderate temperature (20-25°C), suitable relative humidity (55-60%), and standard light cycle (12-h light/dark) in a pathogen-free animal facility. These mice were bred at the Animal Facility of the Soochow University. The 6-week-old *ApoM*$^{-/-}$(n=22) and WT(n=21) mice were fed a high-fat diet (10% lard, 10% milk, 20% cholesterol) for 34 weeks and subjected to a 5 h fasting period prior to sacrifice [31]. Blood glucose level detection and insulin tolerance test were carried out at the 7th and 14th week of high-fat diet (n=17, respectively). At the 23rd week of the high-fat diet, 5 and 4 from these *ApoM*$^{-/-}$ and WT mice were sacrificed for the measurement of glucose metabolism and RNA microarray assay. Rest of the mice kept feeding for the detection of AKT phosphorylation.

2.2. Measurement of the Liver Metabolic Profiles

The liver tissues of mice were removed immediately and washed in cold PBS, snap-frozen in liquid nitrogen, and stored at -80°C until further analysis. Glucose metabolites were extracted from the liver histiocyte lysate using a modified version of the Bligh and Dyer's method [32]. Targeted metabolite profiling was performed on an exion ultra-performance liquid chromatography system (UPLC) coupled with Sciex 6500 Plus Qtrap (Sciex) as described previously [33-35].

2.3. Microarray Analysis for Differentially Expressed mRNAs

The mouse GeneChip® Clariom™ D Array was employed to investigate the liver gene expression profiles of *ApoM*$^{-/-}$ mice, which was purchased by Genechem Co., Ltd. This array provides comprehensive coverage of the mouse genome in a cartridge array format designed for use with the GeneChip® Scanner 3000 7G series. The raw microarray data were applied to the Genespring GX predictor algorithm (Santa Clara) for analysis. The qualified data were normalized by the RMA algorithm and subsequently log-transformed followed by median-subtraction [36]. The gene expression data were processed with the unpaired *t*-test in order to identify the differentially expressed genes and the false discovery rate (FDR) was calculated by the Benjamini-Hochberg method [37]. The genes were regarded as differentially expressed when their *P*-value was less than 0.05 and their fold change was higher than 1.2.

2.4. Glucose Measurements and Insulin Tolerance Test

After 14 weeks of high-fat diet, the *ApoM*$^{-/-}$ and WT mice (n=17) were subjected to fasting for 5 h and then injected with insulin (Humulin R, 0.5 U/kg body weight; Lilly) intraperitoneally in order to analyze insulin tolerance. The tail blood glucose levels were measured prior to the administration of insulin, and at 15, 45, 60, 90, 120, 150 and 180 min following the administration of insulin using a glucose monitor device (Johnson & Johnson, USA).

2.5. Western Blotting

The total protein of the murine muscle, liver and adipose tissues was prepared using the E.Z.N.A DNA/RNA/Protein Isolation Kit (Omega). Western blotting was performed using the following antibodies: anti-AKT (cat. no. 4691; Cell Signaling Technology), anti-phospho-AKT (cat. no. 4060; CST); anti-tubulin (cat. no. ab6160; Abcam); anti-β actin (cat. no. 7077; CST).

2.6. Statistical Analysis

The data are shown as mean ± SEM. The differences between the two groups were evaluated using an unpaired Student's *t*-test. The statistical differences in the volcano map were assessed with the Tukey's HSD test. The scale bar in the heat map indicated the Z-score of the transformed and normalized data corresponding to the concentration of the metabolites. All the calculations were performed using

GraphPad Prism 8.0 (GraphPad Software, Inc.). *P* values less than 0.05 were used for significant differences.

3. RESULTS

3.1. Metabolite Profile of Glucose Metabolism in *ApoM*$^{-/-}$ Mice

A total of 5 and 4 *ApoM*$^{-/-}$ and WT mice were selected respectively for this analysis. The mice were fed a high-fat diet for 23 weeks. The blood glucose level of the *ApoM*$^{-/-}$ mice was higher than that of the WT mice (Fig. **1a** and **1b**) indicated that erythrose-4-phosphate, ribulose-5-phosphate and phosphoenolpyruvate (red plots) exceeded the threshold (P<0.05 and Fold change>1). The data in Fig. (**1c** and **d**) provided an overview of the metabolite changes in the liver tissues of the *ApoM*$^{-/-}$ mice. The majority of the metabolites from the 16 classes of compounds that were detected by UPLC exhibited lower levels in the *ApoM*$^{-/-}$ mice. These were mainly involved in glycolysis, glucuronidation, pentose-phosphate pathway and nucleic acid metabolism. In particular, we focused on the 6 classes of metabolites with statistically significant changes. These were glucose, glucose-6-phosphate (G6P), ribose, ribulose-5-phosphate, erythrose-4-phosphate and adenosine monophosphate (AMP).

3.2. Microarray Profiling of mRNAs in *ApoM*$^{-/-}$ Mice

The mouse GeneChip® Clariom™ D Array was applied to profile the expression levels of mRNAs in *ApoM*$^{-/-}$ and

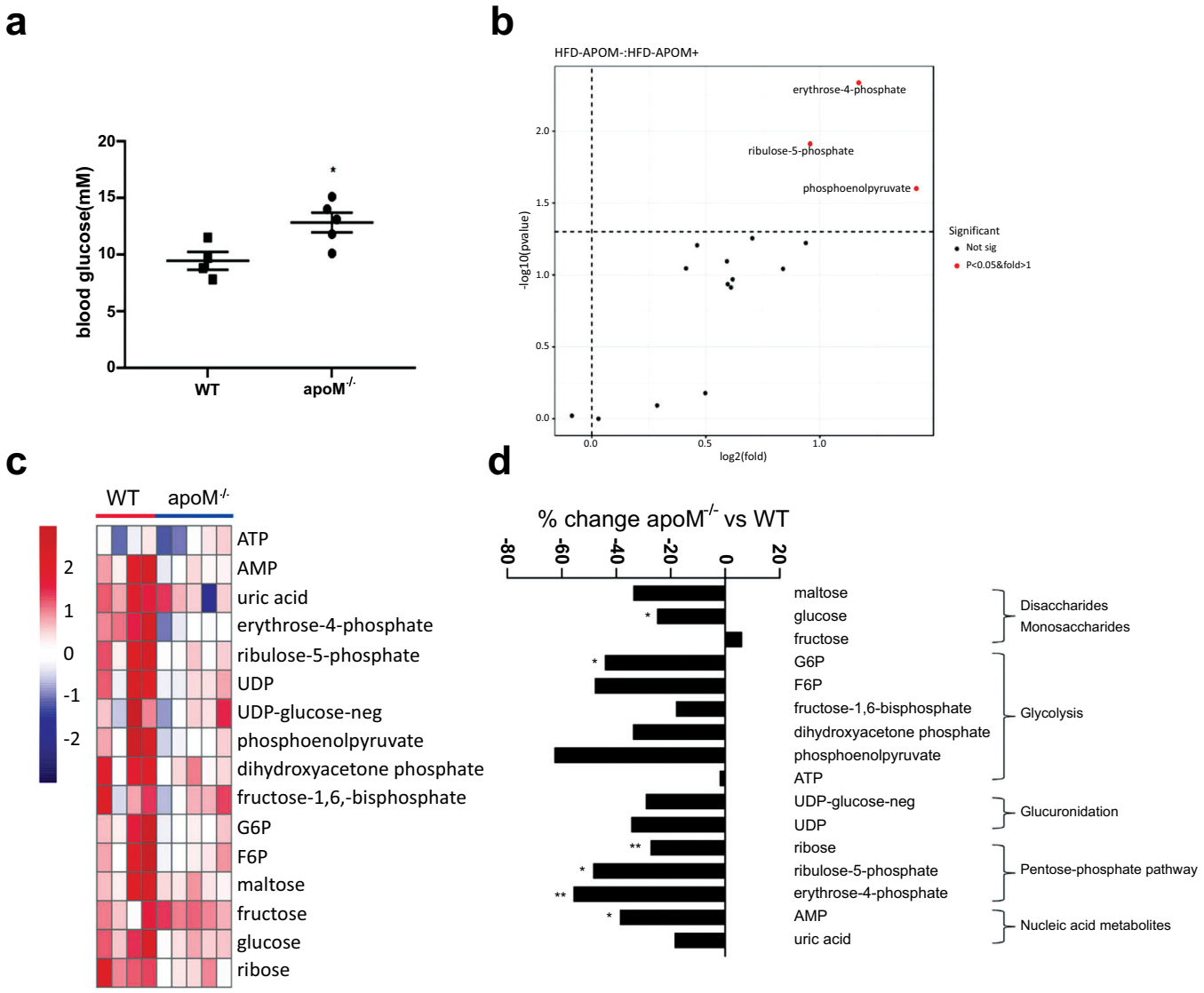

Fig. (1). Glucose related metabolite changes in liver extracts of *ApoM*$^{-/-}$ mice.
(**a**) Blood glucose levels of *ApoM*$^{-/-}$ and WT mice after 23-week high-fat diet (n=4 and 5, Student's *t* test, *p<0.05). (**b**) Volcano map of glucose-related metabolite changes in liver extracts of *ApoM*$^{-/-}$ mice after 23 weeks of high-fat diet (n=4 and 5). The volcano map shows both the *p*-value and the multiples of each variable. Variables that exceed the set threshold are marked (red plots). (Tukey HSD, p<0.05). (**c**) Heat map of glucose-related metabolite changes. The red color and blue color indicate high and low level, respectively.(**d**) % change of glucose-related metabolites in *ApoM*$^{-/-}$ mice *vs* WT. (n=4 and 5). % change = 100 × (up-fold change - 1) or 100 × (1- down-fold change). (Student's *t*-test, *p<0.05, **p<0.01).

WT mice following 23 weeks of a high-fat diet. The quality of microarray data was validated and the Volcano and Scatter plots are depicted in Fig. (**2a** and **b**), respectively. The volcano plot was used for assessing gene expression variation between *ApoM*$^{-/-}$ and WT mice. The scatter plot exhibited the distribution of the signals between *ApoM*$^{-/-}$ and WT mice in the Cartesian coordinate plane. The hierarchical clustering of the genes produced a dendrogram and the heat map was used for analyzing and visualizing microarray data [38] (Fig. **2c**).

A total of 1,134 and 950 from 2,084 mRNAs were categorised as high-expressed and low-expressed (*ApoM*$^{-/-}$ vs WT), respectively. The top 10 differentially expressed genes between the two groups are listed in Table **1**. The data suggested that the expression levels of the mRNAs selected in the *ApoM*$^{-/-}$ mice differed from those in the WT mice.

GO function annotation indicated that the enriched differentially expressed genes were mainly related to the following biological processes: cellular response to stress, organic substance and positive regulation of gene expression.

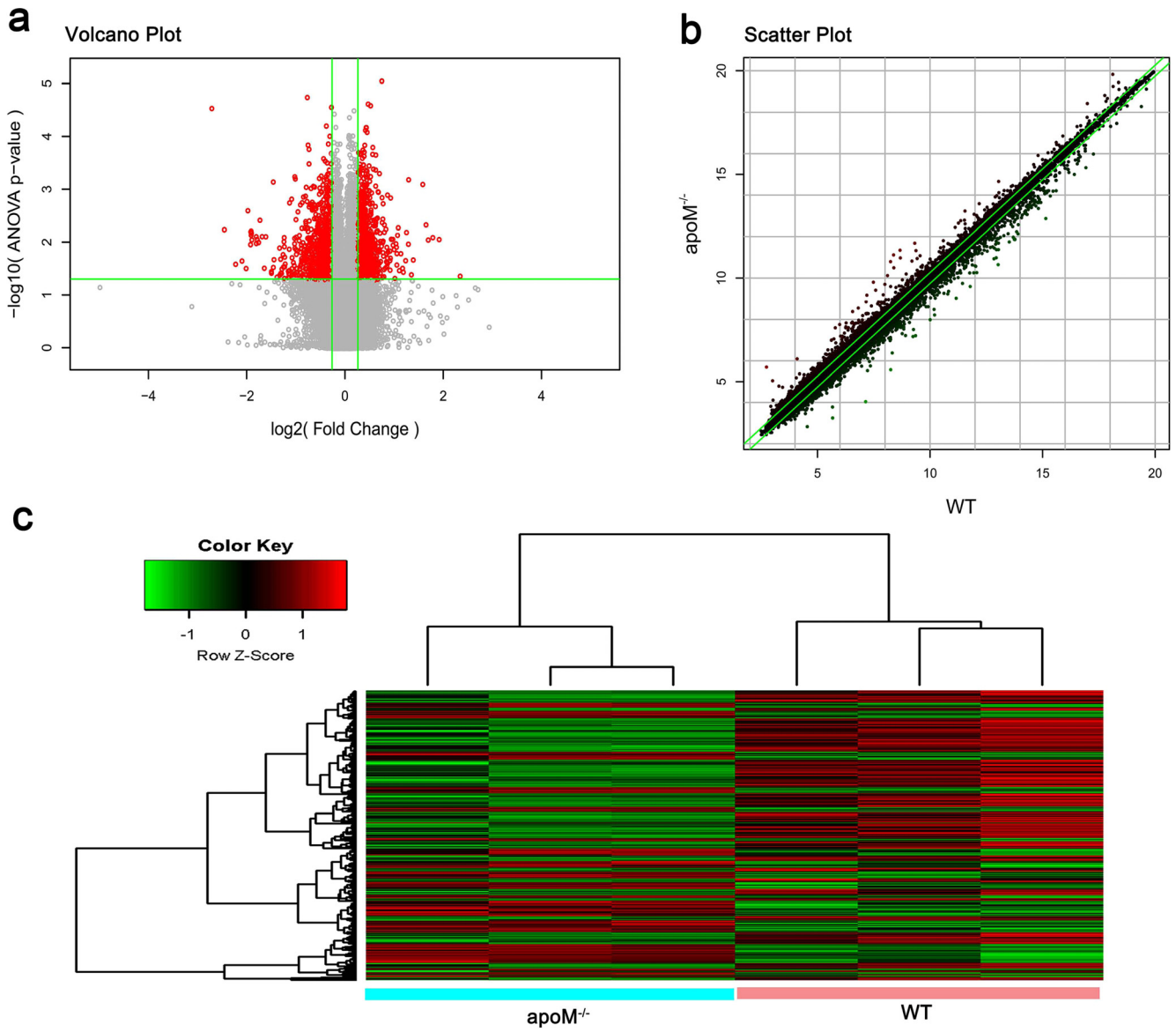

Fig. (2). Screening and clustering of differentially-expressed mRNA between *ApoM*$^{-/-}$ and WT mice. (**a**) Volcano Plot, which demonstrated the distribution of the differentially expressed genes between *ApoM*$^{-/-}$ and WT mice. The X-axis represents the logarithm conversion of the fold difference to base 2 and the Y-axis represents the logarithm conversion of the correct significant levels to base 10. The red color represents all the probes with fold difference >1.2 at a significant level of $p<0.05$. (**b**) Scatter plot, which exhibited the distribution of the signals between *ApoM*$^{-/-}$ and WT mice in a Cartesian coordinate plane. The X-axis represents the WT group, and the Y-axis represents the *ApoM*$^{-/-}$ group. The ordinate value and the abscissa of each spot represent the expression values of one probe in two groups. Red represents the up-regulated genes in *ApoM*$^{-/-}$ group, green represents the up-regulated genes in the WT group, and plots between green parallel lines represent insignificant differentially-expressed genes. (**c**) Clustering diagram of the differentially-expressed RNAs shared in two groups. The color scale represents the different expression of genes from low-to-high, with green representing down-regulated and red representing up-regulated.

Table 1. Top 10 differentially expressed genes between *ApoM*$^{-/-}$ and WT mice.

Gene Symbol	Fold Change	ANOVA *p*-value	Description
Onecut1	3.8037	0.0087	One Cut Homeobox 1
Nudt7	3.1684	0.0046	Nudix Hydrolase 7
Gpcpd1	2.6276	0.0215	Glycerophosphocholine Phosphodiesterase 1
Cish	2.4723	0.0006	Cytokine Inducible SH2 Containing Protein
Slco1a4	2.2923	0.0364	Solute carrier organic anion transporter family member 1A4
Saa1	-4.6466	0.0258	Serum Amyloid A1
Saa2	-4.0098	0.0309	Serum Amyloid A2
Slc41a2	-3.4307	0.0087	Solute Carrier Family 41 Member 2
Nnt	-3.2860	0.0037	Nicotinamide Nucleotide Transhydrogenase
Fgl1	-3.1009	0.0306	Fibrinogen Like 1

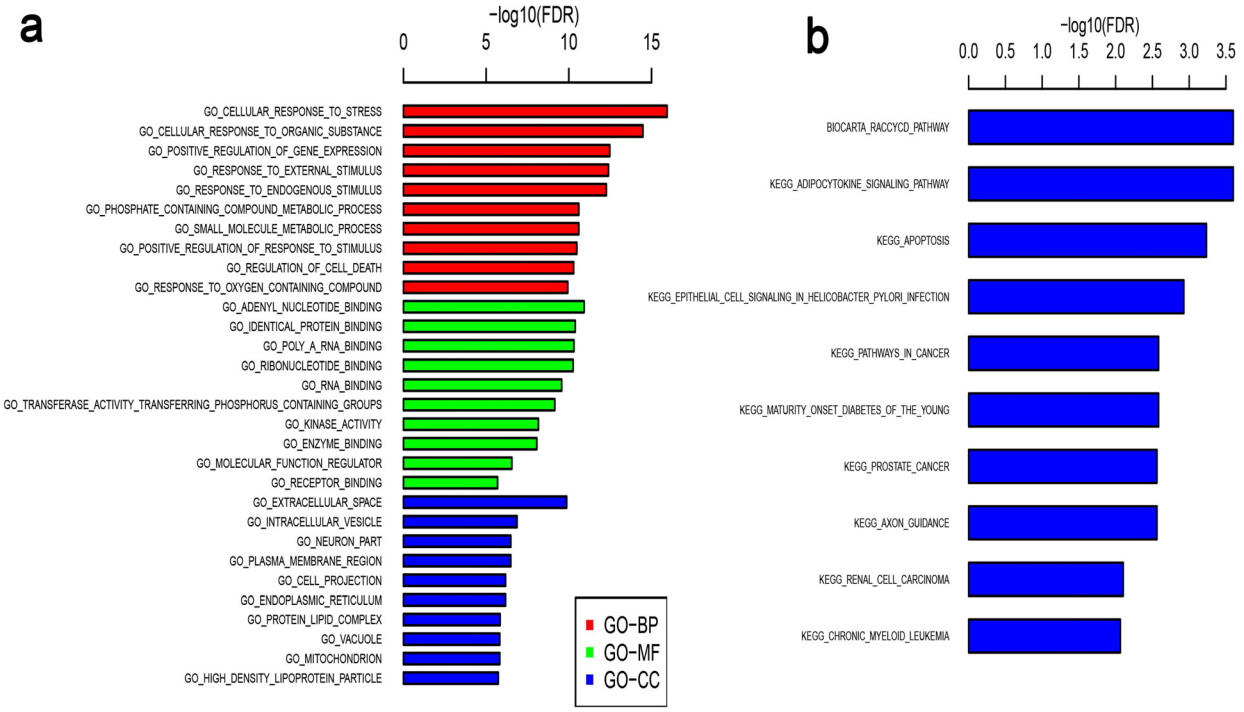

Fig. (3). The Gene Ontology terms and KEGG pathway enrichment of *ApoM*$^{-/-}$ and WT mice. (**a**) GO-BP: Biological process of gene ontology terms. GO-CC: Cellular component of gene ontology terms. GO-MF: Molecular function of Gene Ontology terms. (**b**) KEGG pathways. FDR = false discovery rate.

The GO category of the cellular components was closely associated with extracellular space, intracellular vesicle and neuron. In addition, the differentially expressed genes were significantly enriched in the processes involving adenyl nucleotide binding, identical protein binding and poly-A RNA binding in the GO molecular function module (Fig. **3a**).

Pathway analysis revealed the metabolic pathways undergoing significant changes between the two groups. The data indicated that the differentially-expressed mRNAs were mainly associated with the following signaling pathways: adipocytokine signaling, apoptosis and maturity-onset diabetes of the young (Fig. **3b**). The genes involved in the glucose metabolism pathway are summarized in Table **2**.

3.3. ApoM Improves Insulin Resistance via an AKT-Dependent Mechanism

The *ApoM*$^{-/-}$ and WT mice were fed a high-fat diet for a total of 34 weeks. After 7 weeks of the high-fat diet, the blood glucose levels were significantly higher in *ApoM*$^{-/-}$ mice following 5 h of fasting (Fig. **4a**). The weight loss of the mice was noted in the *ApoM*$^{-/-}$ group at the end of the 29th week compared with that noted in the WT group

Table 2. Genes involved in the glucose metabolism pathway.

Gene Set Name	*p*-value	FDR	Genes in Overlap
Maturity onset diabetes of the young	0.0000329	0.0026	*pklr*
			onecut1
			hhex
			foxa2
ARAP Pathway (ADP-ribosylation factor)	0.000302	0.011	*gbf1*
			cltb
			kdelr2
AKT Signaling Pathway	0.000557	0.0172	*ikbkg*
			akt1
			nfkbia
Pentose and glucuronate interconversions	0.00115	0.0243	*ugt2a1*
			ugp2
			dhdh

FDR = false discovery rate.
Genes in overlap: differential genes overlap in this pathway.

(Fig. **4b**). After 14 weeks of the high-fat diet, an insulin tolerance test was performed to evaluate the modulation of insulin sensitivity. Significant differences were observed between the *ApoM*$^{-/-}$ and the WT mice at 45 min and 60 min, respectively (Fig. **4c**). The sensitivity to insulin was reduced when *ApoM* was knocked out (Fig. **4c**). The AKT phosphorylation levels in the skeletal muscle and adipose tissues were attenuated in *ApoM*$^{-/-}$ mice following insulin injection (Fig. **4d** and **e**) after 34 weeks of the high-fat diet.

4. DISCUSSION

Currently, insufficient evidence has been provided with regard to the association of *ApoM* deficiency with glucose metabolism. In the present study, the data indicated that following a period of high-fat feeding, the blood glucose levels of the *ApoM*$^{-/-}$ mice were significantly higher than those of the WT mice, which was consistent with previous studies [39]. This indicated that in the presence of risk factors for diabetes, apoM demonstrated a protective effect on blood glucose levels. A combination of metabolite profile and microarray analysis in the histiocyte lysate from the mouse liver tissues demonstrated that apoM affected glucose metabolism. Metabolomics is a novel biomedical field used to identify the overall metabolic changes in living organisms [40]. This method provides new insights into the study of diabetes and diabetic complications [41]. Since apoM has been notably studied in liver tissues due to its production by hepatocytes [42, 43], the changes of the glucose metabolites in *ApoM*$^{-/-}$ mice liver were analyzed by metabolomics. Heat map analysis revealed the presence of differentially expressed metabolites, and the results indicated that the majority of these metabolites were reduced in the liver tissues of the *ApoM*$^{-/-}$ mice. Moreover, significant differences were noted in 6 out of the total 16 metabolites, as demonstrated by the unpaired Student's *t*-test. The glucose levels in *ApoM*$^{-/-}$ mice were higher in the blood and lower in the liver tissues. It was hypothesized that this effect may be attributed to the impaired glucose uptake function of *ApoM*$^{-/-}$ liver cells that leads to the accumulation of glucose in the peripheral blood. In addition, G6P is produced by phosphorylation of glucose on the sixth carbon [44]. The decrease in glucose utilization subsequently results in a decrease of G6P formation [45]. Three differential metabolites, namely ribulose-5-phosphate, erythrose-4-phosphate and phosphoenolpyruvate were screened by the Tukey HSD using the following thresholds: $P<0.05$ and fold change>1. The metabolic profile of phosphoenolpyruvate resembled that of G6P, which was also an intermediate product in glycolysis [46]. Ribulose-5-phosphate and erythrose-4-phosphate were intermediate metabolites in the pentose phosphate pathway (PPP) [47]. Their reduction was evident along with the reduction in ribose, suggesting that apoM affected the regulation of the PPP. The PPP is a surrogate pathway of glycolysis and is critical for the synthesis of ribonucleotides comprising a major source of NADPH production [47]. The dehydrogenation from G6P to ribulose 5-phosphate is the first step of the PPP and therefore it is highly possible that the reduction of G6P may trigger the attenuation of the PPP [48]. The present study revealed that the knockout of *ApoM* resulted in the alteration of the glucose metabolite levels in the liver tissues, which subsequently caused glucose-lipid metabolism disorder and eventually led to a series of metabolic diseases, such as diabetes.

In order to further understand the mechanism of these metabolic disorders, bioinformatic analysis was applied to compare differentially expressed mRNAs in the liver tissues

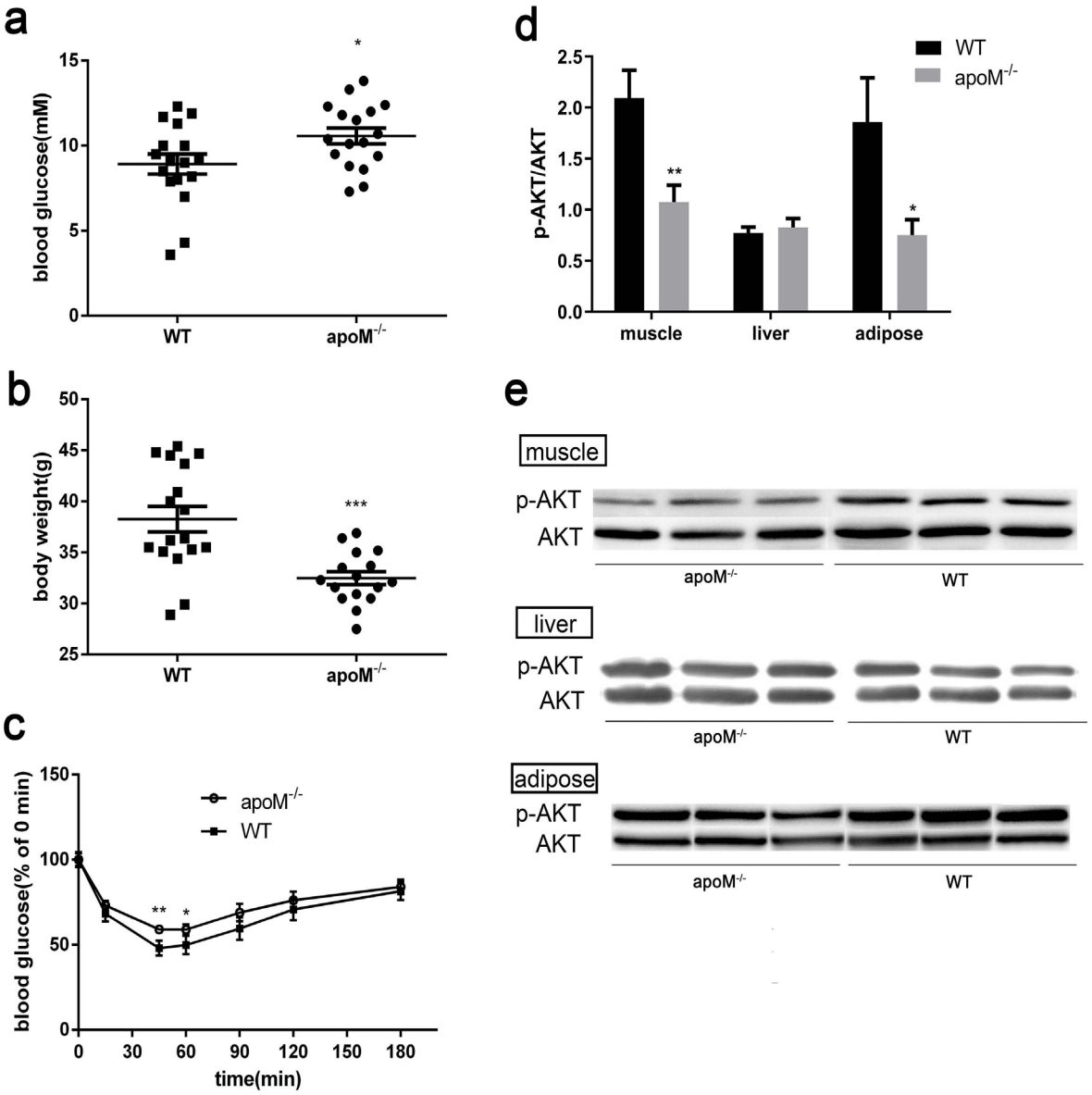

Fig. (4). ApoM improves insulin resistance via AKT-dependent mechanism. (**a**) Blood glucose levels of *ApoM*$^{-/-}$ and WT mice at the 7th week (n=17). (**b**) Bodyweight comparison of *ApoM*$^{-/-}$ and WT mice at the 29th week. (*ApoM*$^{-/-}$: n=16, WT: n=17). (**c**) Insulin tolerance test at the 14th week. Insulin (0.5U/kg body weight) was administered intraperitoneally (n=17). (**d** & **e**) Western blot analysis of phosphorylated Akt (p-Akt) and total Akt (Akt) with homogenates of skeletal muscle (n=15 or 17), liver (n=16) and adipose tissue (n=7 or 8) at the 34th week. The mice were subjected to a 5 h fast, followed by an intraperitoneal injection of 0.5U/kg insulin 30 min prior to euthanization.

of both *ApoM*$^{-/-}$ and WT mice. Volcano and scatter plots were used for assessing gene expression variations between the two groups. Hierarchical clustering analysis demonstrated systematic variations in the expression levels of mRNAs among the samples. The differentially expressed genes were ranked based on the fold change and were listed as the top 10 genes in Table **1**. The first gene in the list was *Onecut1* (*one cut homeobox 1*), also known as *Hnf-6* (*hepatocyte nuclear factor 6*), which is a transcriptional activator of several genes, associated with various regulatory pathways influencing glucose metabolism, cholesterol metabolism, bile acid biosynthesis, as well as the synthesis and transport of serum carrier proteins [49, 50]. HNF-6 is also an important regulator of pancreatic endocrine development [51]. Continuous expression of HNF-6 in mature β-cells leads to loss of pancreatic function and apoptosis [52]. Another differentially expressed gene, namely *Gpcpd1* (*Glycerophosphocholine phosphodiesterase 1*) is also involved in glycerophosphocholine hydrolysis and in skeletal muscle development [53]. The data indicated that the *ApoM* gene defect affected the expression of these differentially expressed genes associated with glucose metabolism. The expression of these genes will be verified by qPCR in the next study thus further exploring their relationship with apoM. GO and KEGG pathway analyses of differentially expressed mRNAs further provided additional information regarding glucose metabolism [54]. All of the differentially expressed mRNAs were utilized for the GO analysis and the results

were summarized in four pathways associated with glucose metabolism (Table **2**). The defect in the *ApoM* gene expression affected the process of the pentose and glucuronate interconversions, which was consistent with the data on glucose metabolism derived from the metabolomic studies. It has been reported previously that type 2 diabetes is associated with lower plasma apoM levels [55]. Moreover, serum apoM levels were suggested as a marker for the mature onset diabetes of the young monogenic forms of diabetes [17]. The results of the present study confirmed genetically that apoM was indeed associated with MODY and that it may be involved in islet cell development via *onecut1*. These findings provided a possible explanation for the different glucose metabolism profiles noted by different mouse genotypes following high-fat diets.

The most important pathway discovered was AKT signaling pathway. Enrichment analysis indicated that the AKT pathway in *ApoM*$^{-/-}$ mice differed from that in WT mice. A previous study has shown that insulin can regulate skeletal muscle and adipose metabolism by promoting glucose transport, glycogen synthesis and protein synthesis by the AKT pathway [56]. Therefore, it was supposed that apoM affected glucose metabolism through AKT pathway. AKT phosphorylation levels were further validated in different tissues. Defects in insulin action within muscle and adipose tissues are common features of insulin resistance [57, 58]. Therefore, insulin was injected into mice as a trigger for observing the activation level of AKT in different tissues [59]. According to the results of the present study, high blood glucose levels and low body weight in *ApoM*$^{-/-}$mice suggested that the absence of apoM increased the risk of developing diabetes in mice. Kurano *et al* reported that overexpression of apoM did not significantly ameliorate insulin sensitivity in WT mice [39], whereas the insulin tolerance test used in the present study suggested that insulin sensitivity was impaired in *ApoM*$^{-/-}$ mice. The phosphorylation levels of AKT in muscle and adipose tissues of *ApoM*$^{-/-}$ mice were significantly diminished in response to insulin stimulation compared with those noted in WT mice (Fig. **4d** and **e**). Although three differentially-expressed genes overlapped in the AKT pathway according to microarray analysis (Table **2**), no significant difference in AKT activation was noted following injection of insulin in the liver tissues. It was assumed that this effect was noted due to the liver being a secondary insulin-sensitive organ [60]. The underlying mechanism requires further investigation.

Further human, animal and cellular experiments are required to substantiate the effects of apoM on glucose metabolism as well as to delineate the mechanisms underlying the association of apoM and T2D, and therefore establish its clinical relevance.

CONCLUSION

In conclusion, the results of the metabolite profile and microarray analysis indicated the presence of glucose metabolism disorders in *ApoM*$^{-/-}$ mice, notably insulin resistance, which eventually resulted in the development of T2D. The *in vivo* experiments of the present study indicated that apoM possibly augmented insulin sensitivity via an AKT-dependent mechanism.

LIST OF ABBREVIATIONS

AKT	=	Protein Kinase B
AMP	=	Adenosine Monophosphate
ApoM	=	Apolipoprotein M
ApoM$^{-/-}$	=	ApoM Deficient
FDR	=	False Discovery Rate
G6P	=	Glucose-6-Phosphate
GO	=	Gene Ontology
Gpcpd1	=	Glycerophosphocholine Phosphodiesterase 1
HDL	=	High-Density Lipoprotein
HNF-1α	=	Hepatocyte Nuclear Factor-1 α
HNF-6	=	Hepatocyte Nuclear Factor 6
KEGG	=	Kyoto Encyclopedia of Genes and Genomes
MODY3	=	Maturity-Onset Diabetes of the Young 3
Onecut1	=	One Cut Homeobox 1
PPP	=	Pentose Phosphate Pathway
T2D	=	Type 2 Diabetes Mellitus
UPLC	=	Ultra-Performance Liquid Chromatography
WT	=	Wild Type

ETHICAL APPROVAL AND CONSENT TO PARTICIPATE

All procedures and animal experiments were approved by the Animal Care and Use Committee of the Soochow University (Suzhou, China) (Approval number: SYXK(Su)2017−0043).

HUMAN AND ANIMAL RIGHTS

No humans were involved in the study. All animal procedures were performed in accordance with the care and use guidelines of the experimental animals of Jiangsu Province, China.

CONSENT FOR PUBLICATION

Not applicable.

AVAILABILITY OF DATA AND MATERIALS

The datasets used and/or analysed during the current study are available from the corresponding authors, [NX and GL], on reasonable request.

FUNDING

This research was supported by the Natural Science Foundation of Jiangsu province (Grant Number: BK20151179), the International Cooperation Foundation of Changzhou (Grant Number: CZ20150012) and the Changzhou High-Level Medical Talents Training Project (Grant Number: 2016ZCLJ002).

CONFLICT OF INTEREST

The authors declare no conflict of interest, financial or otherwise.

ACKNOWLEDGEMENTS

The authors would like to thank Dr. Guanghou Shui (State Key Laboratory of Molecular Developmental Biology, Institute of Genetics and Developmental Biology, Chinese Academy of Sciences, Beijing, China) for providing glucose metabolite analysis in Fig. (**1**).

REFERENCES

[1] Chen, L.; Magliano, D.J.; Zimmet, P.Z. The worldwide epidemiology of type 2 diabetes mellitus--present and future perspectives. *Nat. Rev. Endocrinol.,* **2011**, *8*(4), 228-236. http://dx.doi.org/10.1038/nrendo.2011.183 PMID: 22064493

[2] Jones, J.G. Hepatic glucose and lipid metabolism. *Diabetologia,* **2016**, *59*(6), 1098-1103. http://dx.doi.org/10.1007/s00125-016-3940-5 PMID: 27048250

[3] Xu, H.; Li, X.; Adams, H.; Kubena, K.; Guo, S. Etiology of Metabolic Syndrome and Dietary Intervention. *Int. J. Mol. Sci.,* **2018**, *20*(1), E128. http://dx.doi.org/10.3390/ijms20010128 PMID: 30602666

[4] Rye, K.A.; Barter, P.J.; Cochran, B.J. Apolipoprotein A-I interactions with insulin secretion and production. *Curr. Opin. Lipidol.,* **2016**, *27*(1), 8-13. http://dx.doi.org/10.1097/MOL.0000000000000253 PMID: 26655291

[5] Van Linthout, S.; Foryst-Ludwig, A.; Spillmann, F.; Peng, J.; Feng, Y.; Meloni, M.; Van Craeyveld, E.; Kintscher, U.; Schultheiss, H.P.; De Geest, B.; Tschöpe, C. Impact of HDL on adipose tissue metabolism and adiponectin expression. *Atherosclerosis,* **2010**, *210*(2), 438-444. http://dx.doi.org/10.1016/j.atherosclerosis.2010.01.001 PMID: 20202635

[6] Stenkula, K.G.; Lindahl, M.; Petrlova, J.; Dalla-Riva, J.; Göransson, O.; Cushman, S.W.; Krupinska, E.; Jones, H.A.; Lagerstedt, J.O. Single injections of apoA-I acutely improve *in vivo* glucose tolerance in insulin-resistant mice. *Diabetologia,* **2014**, *57*(4), 797-800. http://dx.doi.org/10.1007/s00125-014-3162-7 PMID: 24442447

[7] McGrath, K.C.; Li, X.H.; Whitworth, P.T.; Kasz, R.; Tan, J.T.; McLennan, S.V.; Celermajer, D.S.; Barter, P.J.; Rye, K.A.; Heather, A.K. High density lipoproteins improve insulin sensitivity in high-fat diet-fed mice by suppressing hepatic inflammation. *J. Lipid Res.,* **2014**, *55*(3), 421-430. http://dx.doi.org/10.1194/jlr.M043281 PMID: 24347528

[8] Poteryaeva, O.N.; Usynin, I.F. [Antidiabetic role of high density lipoproteins]. *Biomed. Khim.,* **2018**, *64*(6), 463-471. http://dx.doi.org/10.18097/PBMC20186406463 PMID: 30632974

[9] Wolfrum, C.; Poy, M.N.; Stoffel, M. Apolipoprotein M is required for prebeta-HDL formation and cholesterol efflux to HDL and protects against atherosclerosis. *Nat. Med.,* **2005**, *11*(4), 418-422. http://dx.doi.org/10.1038/nm1211 PMID: 15793583

[10] Croyal, M.; Billon-Crossouard, S.; Goulitquer, S.; Aguesse, A.; León, L.; Fall, F.; Chétiveaux, M.; Moyon, T.; Blanchard, V.; Ouguerram, K.; Lambert, G.; Nobécourt, E.; Krempf, M. Stable Isotope Kinetic Study of ApoM (Apolipoprotein M). *Arterioscler. Thromb. Vasc. Biol.,* **2018**, *38*(1), 255-261. http://dx.doi.org/10.1161/ATVBAHA.117.310208 PMID: 29146748

[11] Xu, N.; Dahlbäck, B. A novel human apolipoprotein (apoM). *J. Biol. Chem.,* **1999**, *274*(44), 31286-31290. http://dx.doi.org/10.1074/jbc.274.44.31286 PMID: 10531326

[12] Borup, A.; Christensen, P.M.; Nielsen, L.B.; Christoffersen, C. Apolipoprotein M in lipid metabolism and cardiometabolic diseases. *Curr. Opin. Lipidol.,* **2015**, *26*(1), 48-55. http://dx.doi.org/10.1097/MOL.0000000000000142 PMID: 25551802

[13] Christoffersen, C.; Federspiel, C.K.; Borup, A.; Christensen, P.M.; Madsen, A.N.; Heine, M.; Nielsen, C.H.; Kjaer, A.; Holst, B.; Heeren, J.; Nielsen, L.B. The Apolipoprotein M/S1P Axis Controls Triglyceride Metabolism and Brown Fat Activity. *Cell Rep.,* **2018**, *22*(1), 175-188. http://dx.doi.org/10.1016/j.celrep.2017.12.029 PMID: 29298420

[14] Ooi, E.M.; Watts, G.F.; Chan, D.C.; Nielsen, L.B.; Plomgaard, P.; Dahlbäck, B.; Barrett, P.H. Association of apolipoprotein M with high-density lipoprotein kinetics in overweight-obese men. *Atherosclerosis,* **2010**, *210*(1), 326-330. http://dx.doi.org/10.1016/j.atherosclerosis.2009.11.024 PMID: 20031132

[15] Niu, N.; Zhu, X.; Liu, Y.; Du, T.; Wang, X.; Chen, D.; Sun, B.; Gu, H.F.; Liu, Y. Single nucleotide polymorphisms in the proximal promoter region of apolipoprotein M gene (apoM) confer the susceptibility to development of type 2 diabetes in Han Chinese. *Diabetes Metab. Res. Rev.,* **2007**, *23*(1), 21-25. http://dx.doi.org/10.1002/dmrr.641 PMID: 16572495

[16] Cervin, C.; Axler, O.; Holmkvist, J.; Almgren, P.; Rantala, E.; Tuomi, T.; Groop, L.; Dahlbäck, B.; Karlsson, E. An investigation of serum concentration of apoM as a potential MODY3 marker using a novel ELISA. *J. Intern. Med.,* **2010**, *267*(3), 316-321. http://dx.doi.org/10.1111/j.1365-2796.2009.02145.x PMID: 19754856

[17] Richter, S.; Shih, D.Q.; Pearson, E.R.; Wolfrum, C.; Fajans, S.S.; Hattersley, A.T.; Stoffel, M. Regulation of apolipoprotein M gene expression by MODY3 gene hepatocyte nuclear factor-1alpha: haploinsufficiency is associated with reduced serum apolipoprotein M levels. *Diabetes,* **2003**, *52*(12), 2989-2995. http://dx.doi.org/10.2337/diabetes.52.12.2989 PMID: 14633861

[18] Sramkova, V.; Berend, S.; Siklova, M.; Caspar-Bauguil, S.; Carayol, J.; Bonnel, S.; Marques, M.; Decaunes, P.; Kolditz, C.I.; Dahlman, I.; Arner, P.; Stich, V.; Saris, W.H.M.; Astrup, A.; Valsesia, A.; Rossmeislova, L.; Langin, D.; Viguerie, N.; Apolipoprotein, M. Apolipoprotein M: a novel adipokine decreasing with obesity and upregulated by calorie restriction. *Am. J. Clin. Nutr.,* **2019**, *109*(6), 1499-1510. http://dx.doi.org/10.1093/ajcn/nqy331 PMID: 30869115

[19] Yang, L.; Li, T.; Zhao, S.; Zhang, S. Expression of apolipoprotein M and its association with adiponectin in an obese mouse model. *Exp. Ther. Med.,* **2019**, *18*(3), 1685-1692. http://dx.doi.org/10.3892/etm.2019.7755 PMID: 31410126

[20] Lee, M.; Kim, J.I.; Choi, S.; Jang, Y.; Sorn, S.R. The effect of apoM polymorphism associated with HDL metabolism on obese korean adults. *J. Nutrigenet. Nutrigenomics,* **2016**, *9*(5-6), 306-317. http://dx.doi.org/10.1159/000455948 PMID: 28245483

[21] Huang, X.; Liu, G.; Guo, J.; Su, Z. The PI3K/AKT pathway in obesity and type 2 diabetes. *Int. J. Biol. Sci.,* **2018**, *14*(11), 1483-1496. http://dx.doi.org/10.7150/ijbs.27173 PMID: 30263000

[22] Cignarelli, A.; Genchi, V.A.; Perrini, S.; Natalicchio, A.; Laviola, L.; Giorgino, F. Insulin and insulin receptors in adipose tissue development. *Int. J. Mol. Sci*., **2019**, *20*(3), 759. http://dx.doi.org/10.3390/ijms20030759 PMID: 30754657

[23] Haeusler, R.A.; McGraw, T.E.; Accili, D. Biochemical and cellular properties of insulin receptor signalling. *Nat. Rev. Mol. Cell Biol.,* **2018**, *19*(1), 31-44. http://dx.doi.org/10.1038/nrm.2017.89 PMID: 28974775

[24] Boucher, J.; Kleinridders, A.; Kahn, C.R. Insulin receptor signaling in normal and insulin-resistant states. *Cold Spring Harb. Perspect. Biol.,* **2014**, *6*(1)a009191 http://dx.doi.org/10.1101/cshperspect.a009191 PMID: 24384568

[25] Petersen, M.C.; Shulman, G.I. Mechanisms of Insulin Action and Insulin Resistance. *Physiol. Rev.,* **2018**, *98*(4), 2133-2223. http://dx.doi.org/10.1152/physrev.00063.2017 PMID: 30067154

[26] Zheng, Z.; Zeng, Y.; Zhu, X.; Tan, Y.; Li, Y.; Li, Q.; Yi, G. ApoM-S1P Modulates Ox-LDL-Induced Inflammation Through the PI3K/Akt Signaling Pathway in HUVECs. *Inflammation,* **2019**, *42*(2), 606-617. http://dx.doi.org/10.1007/s10753-018-0918-0 PMID: 30377890

[27] Christoffersen, C.; Obinata, H.; Kumaraswamy, S.B.; Galvani, S.; Ahnström, J.; Sevvana, M.; Egerer-Sieber, C.; Muller, Y.A.; Hla, T.; Nielsen, L.B.; Dahlbäck, B. Endothelium-protective sphingosine-1-phosphate provided by HDL-associated apolipoprotein M. *Proc. Natl. Acad. Sci. USA,* **2011**, *108*(23), 9613-9618. http://dx.doi.org/10.1073/pnas.1103187108 PMID: 21606363

[28] Zhu, Y.; Luo, G.; Jiang, B.; Yu, M.; Feng, Y.; Wang, M.; Xu, N.; Zhang, X. Apolipoprotein M promotes proliferation and invasion in non-small cell lung cancers via upregulating S1PR1 and activating the ERK1/2 and PI3K/AKT signaling pathways. *Biochem. Biophys. Res. Commun.,* **2018**, *501*(2), 520-526. http://dx.doi.org/10.1016/j.bbrc.2018.05.029 PMID: 29750961

[29] Wang, Z.; Luo, G.; Feng, Y.; Zheng, L.; Liu, H.; Liang, Y.; Liu, Z.; Shao, P.; Berggren-Söderlund, M.; Zhang, X.; Xu, N. Decreased splenic CD4(+) T-lymphocytes in apolipoprotein M gene deficient mice. *BioMed Res. Int.,* **2015**, *2015*, 293512. http://dx.doi.org/10.1155/2015/293512 PMID: 26543853

[30] Yu, Y.; Zheng, L.; Liang, Y.; Pan, L.; Zhang, J.; Wei, J.; Yu, M.; Luo, G. Establishment of duplex fluorescence RT-PCR for identification of apolipoprotein M gene knockout mice. *Chin J Clin Lab Sci,* **2015**, *33*(6), 412-414.

[31] Surwit, R.S.; Kuhn, C.M.; Cochrane, C.; McCubbin, J.A.; Feinglos, M.N. Diet-induced type II diabetes in C57BL/6J mice. *Diabetes,* **1988**, *37*(9), 1163-1167. http://dx.doi.org/10.2337/diab.37.9.1163 PMID: 3044882

[32] Sündermann, A.; Eggers, L.F.; Schwudke, D. Liquid Extraction: Bligh and Dyer.*Encyclopedia of Lipidomics*; Wenk, M.R., Ed.; Springer Netherlands: Dordrecht, **2016**, pp. 1-4. http://dx.doi.org/10.1007/978-94-007-7864-1_88-1

[33] Lam, S.M.; Wang, Z.; Li, J.; Huang, X.; Shui, G. Sequestration of polyunsaturated fatty acids in membrane phospholipids of Caenorhabditis elegans dauer larva attenuates eicosanoid biosynthesis for prolonged survival. *Redox Biol.,* **2017**, *12*, 967-977. http://dx.doi.org/10.1016/j.redox.2017.05.002 PMID: 28499251

[34] Vinnakota, K.C.; Pannala, V.R.; Wall, M.L.; Rahim, M.; Estes, S.K.; Trenary, I.; O'Brien, T.P.; Printz, R.L.; Reifman, J.; Shiota, M.; Young, J.D.; Wallqvist, A. Network Modeling of Liver Metabolism to Predict Plasma Metabolite Changes During Short-Term Fasting in the Laboratory Rat. *Front. Physiol.,* **2019**, *10*, 161. http://dx.doi.org/10.3389/fphys.2019.00161 PMID: 30881311

[35] Ho, J.E.; Larson, M.G.; Vasan, R.S.; Ghorbani, A.; Cheng, S.; Rhee, E.P.; Florez, J.C.; Clish, C.B.; Gerszten, R.E.; Wang, T.J. Metabolite profiles during oral glucose challenge. *Diabetes,* **2013**, *62*(8), 2689-2698. http://dx.doi.org/10.2337/db12-0754 PMID: 23382451

[36] Fang, Q.; Yao, S.; Luo, G.; Zhang, X. Identification of differentially expressed genes in human breast cancer cells induced by 4-hydroxyltamoxifen and elucidation of their pathophysiological relevance and mechanisms. *Oncotarget,* **2017**, *9*(2), 2475-2501. PMID: 29416786

[37] Ferreira, J.A. The Benjamini-Hochberg method in the case of discrete test statistics. *Int. J. Biostat.,* **2007**, *3*(1), 11. http://dx.doi.org/10.2202/1557-4679.1065 PMID: 22550651

[38] Shannon, W.; Culverhouse, R.; Duncan, J. Analyzing microarray data using cluster analysis. *Pharmacogenomics,* **2003**, *4*(1), 41-52. http://dx.doi.org/10.1517/phgs.4.1.41.22581 PMID: 12517285

[39] Kurano, M.; Hara, M.; Tsuneyama, K.; Sakoda, H.; Shimizu, T.; Tsukamoto, K.; Ikeda, H.; Yatomi, Y. Induction of insulin secretion by apolipoprotein M, a carrier for sphingosine 1-phosphate. *Biochim. Biophys. Acta,* **2014**, *1841*(9), 1217-1226. http://dx.doi.org/10.1016/j.bbalip.2014.05.002 PMID: 24814049

[40] Roberts, L. D.; Souza, A. L.; Gerszten, R. E.; Clish, C. B. Targeted Metabolomics. *Curr. Protoc. Mol. Biol.,* **2012**, *98*(1), 30.2.1-30.2.24. http://dx.doi.org/10.1002/0471142727.mb3002s98

[41] Bain, J.R.; Stevens, R.D.; Wenner, B.R.; Ilkayeva, O.; Muoio, D.M.; Newgard, C.B. Metabolomics applied to diabetes research: moving from information to knowledge. *Diabetes,* **2009**, *58*(11), 2429-2443. http://dx.doi.org/10.2337/db09-0580 PMID: 19875619

[42] Luo, G.; Feng, Y.; Zhang, J.; Mu, Q.; Shi, Y.; Qin, L.; Zheng, L.; Berggren-Söderlund, M.; Nilsson-Ehle, P.; Zhang, X.; Xu, N. Rosiglitazone enhances apolipoprotein M (Apom) expression in rat's liver. *Int. J. Med. Sci.,* **2014**, *11*(10), 1015-1021. http://dx.doi.org/10.7150/ijms.8330 PMID: 25136257

[43] Ren, K.; Tang, Z.L.; Jiang, Y.; Tan, Y.M.; Yi, G.H.; Apolipoprotein, M. Apolipoprotein M. *Clin. Chim. Acta,* **2015**, *446*, 21-29. http://dx.doi.org/10.1016/j.cca.2015.03.038 PMID: 25858547

[44] Adeva-Andany, M.M.; Pérez-Felpete, N.; Fernández-Fernández, C.; Donapetry-García, C.; Pazos-García, C. Liver glucose metabolism in humans. *Biosci. Rep.,* **2016**, *36*(6), e00416. http://dx.doi.org/10.1042/BSR20160385 PMID: 27707936

[45] Froissart, R.; Piraud, M.; Boudjemline, A.M.; Vianey-Saban, C.; Petit, F.; Hubert-Buron, A.; Eberschweiler, P.T.; Gajdos, V.; Labrune, P. Glucose-6-phosphatase deficiency. *Orphanet J. Rare Dis.,* **2011**, *6*, 27. http://dx.doi.org/10.1186/1750-1172-6-27 PMID: 21599942

[46] Schormann, N.; Hayden, K. L.; Lee, P.; Banerjee, S.; Chattopadhyay, D. *An overview of structure, function, and regulation of pyruvate kinases*; , **2019**. http://dx.doi.org/10.1002/pro.3691

[47] Kruger, N.J.; von Schaewen, A. The oxidative pentose phosphate pathway: structure and organisation. *Curr. Opin. Plant Biol.,* **2003**, *6*(3), 236-246. http://dx.doi.org/10.1016/S1369-5266(03)00039-6 PMID: 12753973

[48] Stincone, A.; Prigione, A.; Cramer, T.; Wamelink, M.M.; Campbell, K.; Cheung, E.; Olin-Sandoval, V.; Grüning, N.M.; Krüger, A.; Tauqeer Alam, M.; Keller, M.A.; Breitenbach, M.; Brindle, K.M.; Rabinowitz, J.D.; Ralser, M. The return of metabolism: biochemistry and physiology of the pentose phosphate pathway. *Biol. Rev. Camb. Philos. Soc.,* **2015**, *90*(3), 927-963. http://dx.doi.org/10.1111/brv.12140 PMID: 25243985

[49] Wang, K.; Holterman, A.X. Pathophysiologic role of hepatocyte nuclear factor 6. *Cell. Signal.,* **2012**, *24*(1), 9-16. http://dx.doi.org/10.1016/j.cellsig.2011.08.009 PMID: 21893194

[50] Zhang, Y.; Fang, B.; Damle, M.; Guan, D.; Li, Z.; Kim, Y.H.; Gannon, M.; Lazar, M.A. HNF6 and Rev-erbα integrate hepatic lipid metabolism by overlapping and distinct transcriptional mechanisms. *Genes Dev.,* **2016**, *30*(14), 1636-1644. http://dx.doi.org/10.1101/gad.281972.116 PMID: 27445394

[51] Kropp, P.A.; Dunn, J.C.; Carboneau, B.A.; Stoffers, D.A.; Gannon, M. Cooperative function of Pdx1 and Oc1 in multipotent pancreatic progenitors impacts postnatal islet maturation and adaptability. *Am. J. Physiol. Endocrinol. Metab.,* **2018**, *314*(4), E308-E321. http://dx.doi.org/10.1152/ajpendo.00260.2017 PMID: 29351489

[52] Gannon, M.; Ray, M.K.; Van Zee, K.; Rausa, F.; Costa, R.H.; Wright, C.V. Persistent expression of HNF6 in islet endocrine cells causes disrupted islet architecture and loss of beta cell function. *Development,* **2000**, *127*(13), 2883-2895. PMID: 10851133

[53] Okazaki, Y.; Ohshima, N.; Yoshizawa, I.; Kamei, Y.; Mariggiò, S.; Okamoto, K.; Maeda, M.; Nogusa, Y.; Fujioka, Y.; Izumi, T.; Ogawa, Y.; Shiro, Y.; Wada, M.; Kato, N.; Corda, D.; Yanaka, N. A novel glycerophosphodiester phosphodiesterase, GDE5, controls skeletal muscle development via a non-enzymatic mechanism. *J. Biol. Chem.,* **2010**, *285*(36), 27652-27663. http://dx.doi.org/10.1074/jbc.M110.106708 PMID: 20576599

[54] Huang, W.; Sherman, B.T.; Lempicki, R.A. Systematic and integrative analysis of large gene lists using DAVID bioinformatics resources. *Nat. Protoc.,* **2009**, *4*(1), 44-57. http://dx.doi.org/10.1038/nprot.2008.211 PMID: 19131956

[55] Plomgaard, P.; Dullaart, R.P.; de Vries, R.; Groen, A.K.; Dahlbäck, B.; Nielsen, L.B. Apolipoprotein M predicts pre-beta-HDL formation: studies in type 2 diabetic and nondiabetic subjects. *J. Intern. Med.,* **2009**, *266*(3), 258-267. http://dx.doi.org/10.1111/j.1365-2796.2009.02095.x PMID: 19457058

[56] Saltiel, A.R.; Kahn, C.R. Insulin signalling and the regulation of glucose and lipid metabolism. *Nature,* **2001**, *414*(6865), 799-806. http://dx.doi.org/10.1038/414799a PMID: 11742412

[57] Kubota, T.; Kubota, N.; Kadowaki, T. Imbalanced insulin actions in obesity and type 2 diabetes: Key mouse models of insulin signaling pathway. *Cell Metab.,* **2017**, *25*(4), 797-810. http://dx.doi.org/10.1016/j.cmet.2017.03.004 PMID: 28380373

[58] Lo, K.A.; Labadorf, A.; Kennedy, N.J.; Han, M.S.; Yap, Y.S.; Matthews, B.; Xin, X.; Sun, L.; Davis, R.J.; Lodish, H.F.; Fraenkel, E. Analysis of *in vitro* insulin-resistance models and their physiological relevance to *in vivo* diet-induced adipose insulin resistance. *Cell Rep.,* **2013**, *5*(1), 259-270. http://dx.doi.org/10.1016/j.celrep.2013.08.039 PMID: 24095730

[59] Wang, C.Y.; Liao, J.K. A mouse model of diet-induced obesity and insulin resistance. *Methods Mol. Biol.,* **2012**, *821*, 421-433. http://dx.doi.org/10.1007/978-1-61779-430-8_27 PMID: 22125082

[60] Girard, J. The inhibitory effects of insulin on hepatic glucose production are both direct and indirect. *Diabetes,* **2006**, *55*, S65-S69. http://dx.doi.org/10.2337/db06-S009